Research Square

Preprints are preliminary reports that have not undergone peer review.
They should not be considered conclusive, used to inform clinical practice,
or referenced by the media as validated information.

ONAC103 isoforms generated by alternative promoter coordinately regulate leaf senescence in rice

Shuo An
Fudan University
Yue Hu
Fudan University
Xuan Cheng
Fudan University
Xiaochun Ge
xcge@fudan.edu.cn

Fudan University

Research Article

Keywords: rice, ONAC103, transcription factor, alternative promoter usage, leaf senescence

Posted Date: August 5th, 2026

DOI: https://doi.org/10.21203/rs.3.rs-10457841/v1

License: This work is licensed under a Creative Commons Attribution 4.0 International License.
Read Full License

Additional Declarations: No competing interests reported.

Abstract

Leaf senescence is a developmentally programmed degenerative process essential for nutrient remobilization from aging leaves to sink organs, thereby enhancing plant fitness and reproductive success. This process is governed by a complex regulatory network integrating developmental age, endogenous signals and environmental cues, and its molecular mechanisms remain incompletely elucidated. In this study, we found that *ONAC103*, a gene encoding NAC-family transcription factor, exhibits dual regulatory functions in leaf senescence through alternative promoter usage. A truncated RNA isoform, named *ONAC103S* was identified in addition to the canonical full length *ONAC103L* isoform. *ONAC103S* is driven by an intronic promoter and lacks the N-terminal NAC domain of ONAC103L. Both *ONAC103L* and *ONAC103S* can be upregulated by leaf senescence, abiotic stress and ABA treatment but with different temporal expression patterns. ONAC103L acts as a senescence accelerator, whereas ONAC103S counteracts ONAC103L activity during late leaf aging stages. *ONAC103S*-overexpression lines displayed the same phenotype of delayed senescence as *onac103* mutants. Dual-luciferase assay, ChIP-qPCR and EMSA results confirmed that ONAC103L directly binds to the promoters of senescence-associated genes such as *OsPAO, OsNOL, OsNAP*, and *OsNYC4*, and activates their expressions, while ONAC103S competitively inhibits the transcriptional activation activity of ONAC103L on downstream genes. This antagonistic interaction establishes a negative feedback loop to attenuate senescence progression. Our findings unveil a novel dual regulatory mechanism where ONAC103 produces antagonistic isoforms through alternative promoter usage: the full-length protein initiates senescence, while its truncated counterpart contributes to termination of this process. This bimodal regulation may ensure precise and fine temporal control over senescence progression in rice.

Introduction

Leaf senescence is a genetically programmed developmental process that signifies the final stage in the life cycle of plant leaves. It is characterized by the dismantling of chloroplast ultrastructure and the catabolic degradation of chlorophyll, which results in progressive leaf yellowing and eventual wilting (Lim et al. 2007). During this process, a diverse array of senescence-associated genes (SAGs), including chlorophyll catabolic genes (CCGs), are dynamically regulated (Gao et al. 2016; Yu et al. 2022). Given the critical roles of leaf senescence in plant longevity, crop yield, and stress resilience (Guo et al. 2021), dissecting the regulatory networks that coordinate this process is of great scientific importance in plant biology.

NAC transcription factors (TFs) represent one of the largest TF families regulating leaf senescence (Mathew and Agarwal. 2018). Arabidopsis and rice possess 117 and 151 NAC proteins, respectively (Nuruzzaman et al. 2010; Xiong et al. 2025). Based on characterized NAC proteins, a typical NAC TF often contains a conserved N-terminal NAC domain and a variable C-terminal transcriptional regulatory domain (TRD) (Olsen et al. 2005; Xiong et al. 2025). The NAC domain can be subdivided into five functional subdomains (A–E): subdomain A mediates protein homo- or hetero- dimerization; subdomains C and D are highly conserved, positively charged, and responsible for DNA binding; while

subdomains B and E show considerable diversity among NAC members (Xiong et al. 2025). NAC TFs can promote or delay leaf senescence through upregulation or inhibition of target gene expression. For instance, ANAC029/NAC-LIKE, ACTIVATED BY AP3/PI (AtNAP) (Guo and Gan. 2006), ANAC019, ANAC055 and ANAC072 (Zhu et al. 2015), ANAC092/ORESARA 1 (ORE1) (Balazadeh et al. 2010), and ANAC059/ORE1 SISTER 1 (ORS1) (Balazadeh et al. 2011) in *Arabidopsis* promote leaf senescence. In contrast, the “NAC troika” (ANAC017, ANAC082, and ANAC090) (Kim et al. 2018) and ANAC083/VND-INTERACTING2 (VNI2) (Nagahage et al. 2023) act as negative regulators of this process. Genome-wide studies indicate that 57.5% (65 out of 113) of Arabidopsis *NAC* genes are senescence-associated (sen-NACs) (Kim et al. 2018).

Compared to Arabidopsis, only a few NAC proteins have been characterized in rice as being involved in leaf senescence. Positive regulators include OsNAP (Liang et al. 2014), ONAC2 (Mao et al. 2017), ONAC096 (Kang et al. 2019), ONAC011/OsY37 (El Mannai et al. 2017), ONAC103 (Sun et al. 2024), and ONAC054 (Sakuraba et al. 2020). OsNAP is upregulated by ABA but inhibits ABA biosynthesis via an unknown feedback mechanism. It directly binds to CCGs including *SGR*, *NYC1*, *NYC3* and *RCCR*1 to promote chlorophyll degradation (Liang et al. 2014). ONAC2 binds directly to promoters of CCGs including *SGR*, *NYC3* and ABA metabolism-related genes *OsNCED3*, *OsZEP1*, and *OsABA8ox1*, therefore promotes leaf senescence through ABA biosynthesis (Mao et al. 2017). ONAC096 activates *OsNAP* and ABA signaling genes *ABI5* and *EEL (ENHANCED EM LEVEL)* (Kang et al. 2019). ONAC011/OsY37 (Oryza sativa Yellow37) accelerates heading time in addition to leaf senescence, while its downstream target genes remain uncharacterized (El Mannai et al. 2017). A recent study demonstrated that ONAC103 upregulates the expression of SAGs such as *OsSGR* and *OsNYC1* likely through ABA and JA signaling pathways (Sun et al. 2024); however, whether ONAC103 can directly regulate these SAGs remains unclear. Interestingly, the *ONAC054* gene produces two RNA isoforms *ONAC054α* and *ONAC054β* through alternative splicing. ONAC054α contains a C-terminal transmembrane domain (TMD) and is associated with the endoplasmic reticulum (ER) membrane, whereas ONAC054β lacks this TMD and is constitutively nuclear-localized (Sakuraba et al. 2020). ABA triggers the cleavage of ONAC054α’s TMD for nuclear translocation. Both isoforms coordinately mediate ABA-induced leaf senescence through transcriptional activation of *OsABI5* and *NYC1* (Sakuraba et al. 2020). In contrast, only two NAC TFs, including ONAC106 and ONAC109 are found to negatively regulate rice leaf senescence. ONAC106 delays leaf senescence by repressing the expression of *SGR* and *NYC1* (Sakuraba et al. 2015), and ONAC109 functions as a senescence repressor by regulating the expression of multiple hormone-associated genes and SAGs (Li et al. 2021).

Eukaryotes often produce proteins more than their genes. The mechanisms for expanding the diversities of proteomes include alternative splicing, alternative transcription/translation initiation, alternative polyadenylation, and alternative promoter usage (de Klerk and 't Hoen. 2015; Ushijima et al. 2017). Among them, alternative splicing is extensively studied but other mechanisms are rarely characterized, especially in plants. In this study, we identified a previously unreported regulatory paradigm in rice: the *ONAC103* locus generates RNA isoforms through alternative promoter usage. Besides the canonical full-length transcript *ONAC103L*, an intronic promoter drives the transcription of a short RNA isoform

ONAC103S, which produces truncated protein isoforms. Genetic and molecular analyses revealed that ONAC103S function as a dominant-negative regulator by interacting with ONAC103L and suppressing its transcriptional activation of SAGs. These findings uncover a novel post-transcriptional mechanism controlling leaf senescence in rice, and highlight alternative promoter usage as an important regulatory strategy for coordinating developmental programs in plants.

Results

ONAC103 locus produces multiple protein isoforms

Identification and characterization of transcription factors that function in both stress response and leaf senescence are important to fully understand the relationship between these two processes. In a genome-wide profiling study about rice NACs, *ONAC103* expression was shown to be induced by ABA and abiotic stresses (Fang et al. 2008), suggesting that it might be involved in abiotic stress response or leaf senescence. To investigate the function of *ONAC103* in rice, we generated *ONAC103*-overexpresion lines by introducing the genomic DNA fragment and full-length cDNA fragment of *ONAC103*, each fused to a 3×Flag tag, under the transcriptional control of the CaMV 35S promoter into rice plants (*35S: G103-3×Flag* and *35S:C103-3×Flag*, respectively). When identifying the OE lines via western blot analysis, unexpectedly, multiple protein bands were detected in the OE lines harboring the genomic *ONAC103* fragment, with the largest band corresponding to the expected molecular weight of ONAC103 (389 aa, 42.61kD). In contrast, only the predicted ONAC103 band was identified in the OE lines carrying the ONAC103 cDNA fragment. No nonspecific bands were observed in control plants or other transgenic lines lacking ONAC103-3×Flag expression (Fig. 1A). To further confirm these observations, we transiently expressed these constructs in tobacco leaves. Consistent with our initial findings, multiple bands were again detected in samples expressing the genomic construct, whereas only a single band was observed in those expressing the cDNA construct (Fig. 1B). Collectively, these results demonstrate that the additional protein bands originate specifically from the genomic ONAC103 fragment, but not from its cDNA counterpart.

We then analyzed the gene structure of *ONAC103*, and identified a canonical TATA box (TATAATA) and an upstream CAAT box within intron 2 in the *ONAC103* genomic sequence, indicating the potential presence of an intronic promoter in intron 2 (Fig. 1C). To verify its functionality, we constructed two reporter plasmids: *ONAC103pro: GUS*, which contains the native upstream promoter, and *ONAC103ipro: GUS*, in which the intronic promoter sequence was placed upstream of the *GUS* reporter gene. Transient expression assays in tobacco leaves demonstrated that the intronic promoter was functional, albeit with a weaker activity compared to the upstream promoter (Figs. 2A, 2B). Additionally, a dual-luciferase reporter assay in rice protoplasts confirmed that the intronic promoter could drive luciferase reporter gene expression, though its activity was lower than that of the upstream promoter (Fig. 2C).

To determine the transcriptional start sites (TSS) of *ONAC103*, we performed 5’- Rapid amplification of cDNA end (5’-RACE) analysis and identified a full-length isoform (*ONAC103L*), initiating at –109 bp

upstream of its ATG codon and a short isoform (*ONAC103S*), initiating at –70 bp upstream of its putative ATG codon. Typical TATA boxes were found at –21 bp (for *ONAC103L*) and –28 bp (for *ONAC103S*) relative to their respective TSS (Fig. 1C). Based on the information provided by Rice Genome Annotation Project (https://rice.uga.edu), *ONAC103* encodes three alternative splice variants. We then designed primers to amplify *ONAC103*-derived RNA transcripts, and identified two isoforms: the full-length *ONAC103L* (699 bp), which contains all three exons (*ONAC103.1*), and a longer variant (*ONAC103.2*, 779 bp) with intron 1 retention (Fig. S1B). The transcript with the complete intron 2 retention was not detected when amplification spans three exons, consistent with the findings of the previous study (Sun et al. 2024). Importantly, amplification with a primer located downstream of the *ONAC103S* TSS and another primer within exon 3 yielded a product corresponding to the predicted size of *ONAC103S* (Fig. S1C), confirming the *in vivo* existence of *ONAC103S*. *ONAC103S* is driven by a promoter within intron 2, with transcription initiating in this intron, 124 bp upstream of exon 3 (Fig. 1C and Fig. 2A).

Since a 3×Flag tag was fused to the C-terminus of the genomic DNA fragment, the presence of additional protein bands in *35S:G103-3×Flag* transgenic lines indicates that these bands share a common C-terminus with ONAC103L. To determine whether these additional bands generated by the *ONAC103* genomic fragment are derived from the short RNA isoform *ONAC103S*, we expressed the cDNA constructs of *ONAC103L* and *ONAC103S* in tobacco leaves, with the empty vector as a control (Fig. 3A).

Western blot analysis revealed that the *ONAC103L* cDNA directed exclusive expression of the full-length protein. In contrast, the *ONAC103S* cDNA yielded two similarly sized and closely spaced protein bands, which were also observed in the genomic DNA transgenic lines (Fig. 1B). These bands most likely result from leaky ribosomal scanning, owing to the presence of two adjacent ATG start codons within the N-terminus of ONAC103S (designated S1 and S2 in Fig. 1C). Additionally, a prominent low-molecular-weight band was detected, suggesting that the ONAC103S may not be stable when expressed independently. Notably, the combined banding pattern derived from the *ONAC103L* and *ONAC103S* cDNAs closely matched that produced from the genomic ONAC103 fragment (Fig. 3A, 1B). Similar results were also obtained from transgenic rice lines harboring the *ONAC103L* and *ONAC103S* cDNA constructs (Fig. 3B).

The *ONAC103S* transcript encodes the intact transcriptional regulatory (TR) domain of ONAC103L but lacks the major portion of the NAC domain (Fig. 2A). Previous studies have demonstrated that the TR domain of NAC TFs mediates transcriptional activation (Sun et al. 2024; Xiong et al. 2025). We therefore split ONAC103 into N-terminal NAC domain and C-terminal TR domain, and confirmed that the TR domain can activate reporter gene transcription (Fig. S2). Notably, ONAC103S contains an extra 18 amino acids upstream of the TR domain (Fig. 2A, Fig.S3A). We then assessed the transactivation activity of ONAC103S in yeast. Strikingly, ONAC103S exhibited no transactivation activity (Figs. 4A, 4B). We hypothesized that the loss of activity was attributable to the 18 additional amino acids at the N-terminus of the TR domain. To test this, we fused this 18-aa peptide to other well-characterized transcription factors and demonstrated that the N-terminal 18 aa of ONAC103S are sufficient to repress the

transactivation activity of diverse transcription factors, including members of the bZIP, WRKY, and NAC families (Fig. 4C).

Subcellular localization of proteins encoded by *ONAC103L* and *ONAC103S*

Alternative promoter selection usually provides mechanisms for producing functionally or localizationally distinct protein isoforms, we then determined the subcellular localizations of protein isoforms encoded by *ONAC103S* and *ONAC103L*. Transient expression of eGFP-tagged ONAC103L and ONAC103S in rice protoplasts revealed that ONAC103L localized exclusively to the nucleus, whereas ONAC103S protein isoforms were detected in both the cytoplasm and nucleus (Fig. 4D). To investigate the structural basis underlying this differential subcellular localization, we analyzed the nuclear localization signals (NLS) and nuclear export signals (NES) in ONAC103L and the ONAC103S isoforms. Both RNA isoforms were predicted to encode the same NLS (Figs. S3A-B), while ONAC103S harbors a strong NES at its N-terminus, which is embedded in the N-terminal 18 amino acids and likely underlies the cytoplasmic signals for ONAC103S. Interestingly, this NES signal is absent in ONAC103L (Fig. S3C).

Expression patterns of *ONAC103L* and *ONAC103S*

To investigate the functions of *ONAC103L* and *ONAC103S* gene isoforms, we analyzed their expression patterns using RT-qPCR with isoform-specific primers. The results revealed distinct induction patterns under various abiotic stresses: *ONAC103L* was induced by NaCl, PEG6000, heat, cold, and oxidative stress, whereas *ONAC103S* exhibited only marginal induction by PEG6000 and high temperature (Fig. 5A). In response to phytohormone treatments, most hormones including gibberellic acid 3 (GA_3), indole-3-acetic acid (IAA), methyl jasmonic acid (MeJA), salicylic acid (SA), and ethylene suppressed *ONAC103L* expression while only having minimal effects on *ONAC103S* (Fig. S4), with ABA induced both isoforms (Fig. 5A). In the first leaf, *ONAC103L* expression was upregulated upon senescence onset, while *ONAC103S* showed a dramatic increase during later senescence stages (Fig. 5B, 5C). This expression pattern was consistently observed in the second rice leaf as well (Figs. 5D, 5E). Under dark-induced senescence conditions, *ONAC103L* transcript levels gradually increased over time, in contrast to *ONAC103S* which showed a sharp induction specifically on day 5 (Figs. 5F, 5G). Tissue-specific expression analysis demonstrated that both isoforms were predominantly expressed in leaves, with higher expression levels in flag leaves compared to seedling leaves (Fig. 5H). Collectively, these findings demonstrate that both *ONAC103L* and *ONAC103S* are induced during natural aging and dark-induced senescence, supporting the crucial role of the *ONAC103* gene locus in leaf aging.

The phenotype of *ONAC103S*-overexpression lines in rice leaf senescence is similar to that of *onac103* mutants.

Previous studies have established that ONAC103L acts as a positive regulator of leaf senescence in rice. Overexpression of *ONAC103L* accelerates leaf senescence, whereas its knockout delays the process (Sun et al. 2024). Our findings are consistent with this observation (Fig. S5). To explore the function of ONAC103S, we generated *ONAC103S*-overexpression lines. Phenotypic analysis showed that these lines

displayed delayed leaf senescence relative to the wild-type ZH11 at both the ripening and seedling stages (Fig. 6A–C and Fig. S6). Under dark-induced senescence conditions, the *ONAC103S*-overexpression lines also showed delayed chlorophyll degradation and reduced leaf yellowing compared to ZH11 (Fig. 6D–F). These phenotypes resemble those of loss-of-function mutants *onc103-1* and *onc103-2* (Fig. S5), and contrast with the accelerated senescence seen in *ONAC103L*-overexpression lines. Together, these genetic data indicate that ONAC103S and ONAC103L play opposing roles in regulating leaf senescence in rice.

ONAC103L positively regulates the expression of *SAGs*

Although ONAC103 has been reported to promote leaf senescence in rice (Sun et al. 2024) , the direct downstream targets have not yet been revealed. To investigate the molecular mechanisms by which the canonical isoform ONAC103L regulates leaf senescence in rice, we harvested the first leaves of ZH11 and *onc103-1* seedlings, respectively, and subjected them to dark-induced senescence. The expression levels of key *SAGs*, particularly *CCGs*, were examined daily. The results revealed that in the *onac103-1* mutant, the expression levels of *OsNYC1*, *OsNYC3*, *OsNYC4*, *OsNOL*, *OsPAO*, *ONAC5*, *OsNTL*, and *OsNAP* were significantly lower than those in ZH11; furthermore, these genes were either not induced or only weakly induced in the mutant (Fig. 7A). Given that *ONAC103L* encodes a transcription factor, we employed a dual-luciferase reporter system to investigate whether ONAC103L can upregulate the promoter activity of these genes. Assay results demonstrated that ONAC103L activates the transcription of *OsNYC4*, *OsNOL*, *OsPAO*, and *OsNAP* (Fig. 7B), but not that of *OsNYC1*, *ONAC3*, *ONAC5*, *or OsNTL*, suggesting that *OsNYC4*, *OsNOL*, *OsPAO*, and *OsNAP* might be the direct downstream targets of ONAC103L.

To characterize the consensus binding sequence of ONAC103, we performed a DNA affinity purification sequencing (DAP-Seq) assay, which identified the consensus sequence ACACGGCACT (Fig. 7C). Its core motif, CACG, is consistent with the previously reported NAC binding site (NACBS) for most NAC proteins (Puranik et al. 2012; Tran et al. 2004). Analysis of the promoter sequences of *OsPAO*, *OsNOL*, *OsNAP* and *OsNYC4* identified multiple CACG core motifs within their regulatory regions (Fig. 8A, C, E, G). We therefore conducted chromatin immunoprecipitation (ChIP)-qPCR assays using transgenic lines expressing ONAC103L-eYFP, which revealed that ONAC103L accumulates in the promoters of these four genes (Figs. 8A, C, E, G), with particular enrichment in regions containing the CACG motif. To validate these interactions, Electrophoretic mobility shift assays (EMSA) was performed using promoter fragments that exhibited high ONAC103L enrichment in the ChIP-qPCR. The results confirmed that ONAC103L directly binds to these fragments (Figs. 8B, D, F, H). Taken together, our findings indicate that ONAC103L directly associates with the promoters of specific SAGs, including *OsPAO*, *OsNOL*, *OsNAP*, and *OsNYC4*, and activates their expression to promote leaf senescence.

ONAC103S inhibits the transcriptional activation activity of ONAC103L

Since ONAC103L and ONAC103S share the common C-terminal TR domain, clarifying their functional relationship is critical. To address this, we first employed a yeast two-hybrid (Y2H) assay to investigate their potential interaction. The results showed that both proteins can form homodimers as well as heterodimers, with the ONAC103L–ONAC103S heterodimer exhibiting stronger interaction than the ONAC103L–ONAC103L homodimer (Figs. 9A, B). Given that *OsPAO*, *OsNOL*, *OsNAP*, and *OsNYC4* have been identified as target genes of ONAC103L, we then introduced *35S:ONAC103L* and *35S:ONAC103S* separately into rice protoplasts and examined the expression levels of these genes. The introduction of *ONAC103L* increased the transcript levels of all four genes, consistent with its role as a transcriptional activator. In contrast, *ONAC103S* expression caused no significant changes (Fig. S7A–D), which can be attributed to its lack of transcriptional activation activity. Notably, co-expression of *35S:ONAC103L* and *35S:ONAC103S* resulted in markedly lower expression levels of all four target genes compared to the expression of *35S:ONAC103L* alone.

Collectively, these findings demonstrate that ONAC103S acts as a dominant-negative regulator that suppresses ONAC103L-mediated transcriptional activation. This conclusion was further confirmed by dual-luciferase reporter assays (Fig. 9C–G). To determine whether this inhibition is direct, we expressed and purified recombinant ONAC103S protein from *E. coli* and performed EMSA to assess its effect on the binding of ONAC103L to the target promoters. The results revealed that ONAC103S alone did not bind to the promoter sequences. However, its presence significantly impeded ONAC103L binding to these regions (Fig. 9H–K).

Discussion

NAC transcription factors have been shown to regulate a wide range of physiological processes (Xiong et al. 2025). They constitute a large TF family in plants and the function of individual transcription factor needs be revealed. In this study, we found that *ONAC103* gene locus produces a short RNA isoform *ONAC103S* driven by an intronic promoter, in addition to the normal long RNA isoform *ONAC103L* driven by the canonical upstream promoter. The long isoform promotes leaf senescence, while the short isoform inhibits the transcriptional activation function of the long isoform and plays a negative role in leaf senescence at the later stage of leaf senescence.

Alternative splicing has been reported to modulate the functions of the characterized NAC transcription factors, such as rice *ONAC054* and *Populus PtRD26*, which utilize this mechanism to generate splice variants with either similar or opposing functions (Sakuraba et al. 2020; Wang et al. 2021). However, alternative promoter usage has been rarely reported for TFs. Intronic alternative promoters are typically located downstream of canonical promoters and drive transcription from intronic transcription start sites (TSSs). This results in protein isoforms with truncated N-termini compared to their canonical counterparts, a feature that may confer distinct functions or subcellular localization. In mammals, misbalance of functionally distinct protein isoforms can cause detrimental consequences such as developmental defects and diseases (Davuluri et al. 2008). In plants, a genome-wide study in *Arabidopsis* show that light induces alternative promoter selection in thousands of genes through the photoreceptor

phytochrome, and generates protein isoforms with different cell localizations from the isoforms under darkness (Ushijima et al. 2017). The bean (*Phaseolus vulgaris*) *PvSR2 (Stress-Related gene number 2*) produces a metal-responsive element (MRE)-binding transcription factor (PvMTF-1) by using an intronic promoter and it binds to MRE residing in the promoter of the host gene, therefore providing a positive regulatory feedback loop of *PvSR2* expression (Qi et al. 2007). A recent study showed that pear *EARLY FLOWERING3* (*PbELF3*) and its *Arabidopsis* homolog, *AtELF3*, utilize alternative promoters. In addition to the full-length *PbELF3α*, a 58-bp sequence within the second intron of *PbELF3* generates the short transcript *PbELF3β*. These two transcripts exert opposing roles in flower induction: *PbELF3β* promotes flowering, while *PbELF3α* delays it (Wang et al. 2023).

The intron 2 region of the *ONAC103* gene locus exhibits typical promoter features, including a canonical TATA and a CAAT box. Both GUS and tobacco luciferase reporter assays confirmed its capability to drive reporter gene expression, and the promoter activity of *ONAC103S* was weaker than that of *ONAC103L* (Fig. 2C), consistent with their relative expression level in plants (Fig. 5). 5'-RACE analysis further revealed that transcription initiates at 28 bp downstream of the TATA box within intron 2 of *ONAC103L*. We also examined the sequence context around the first and second in-frame ATG codons of *ONAC103S*, which are separated by only two amino acids. Both ATGs reside in "adequate" Kozak motifs. In eukaryotes, translation initiation typically requires an AUG codon within an optimal Kozak sequence gccRccAUGG, where the − 3 (a purine, preferably A) and + 4 (G) positions are most critical (Kozak. 1987). According to established classification, motifs possessing only one of these key residues are deemed “adequate” (Hernández et al. 2019). Following this criterion, the first and second ATG of *ONAC103S* both qualify as "adequate motifs," and correspond to the detected protein bands of 27.17 kDa and 26.84 kDa, respectively (Fig. 1A). Notably, expression of ONAC103S alone is more prone to degradation than co-expression of ONAC103S with ONAC103L, suggesting that ONAC103L may help stabilize ONAC103S.

ONAC103S lacks the DNA-binding domain characteristic of NAC TFs but retains the transactivation domain (TRD), and carries an additional 18-amino-acid peptide at the N-terminus of TRD (Fig. 2A and Supplemental Fig. S3), We confirmed that the TRD possesses transcriptional activation activity whereas the presence of this N-terminal extension abolishes the activation activity (Fig. 4A), indicating an inhibitory role of this peptide. This repressive effect was further corroborated by fusing the peptide to other transcription factors, which similarly compromised their activation function (Fig. 4C). Deciphering how this short peptide broadly inactivates diverse TFs will be an interesting issue for future study.

NAC TRDs are intrinsically disordered regions (IDRs) known to mediate both transcriptional activation and protein–protein interactions (Jensen et al. 2010). For example, the barley NAC TF HvNAC013 interacts with the hub protein RCD1 via the C-terminal segment of its TRD (Kjaersgaard et al. 2011), and *Arabidopsis* ANAC013 and ANAC046 similarly associate with AtRCD1 via their highly disordered TRDs (O'Shea et al. 2015). Given that IDRs also facilitate self-association to drive the formation of biomolecular condensates (Liu et al. 2024), it is likely that the TRD of ONAC103 may also be involved in such process. Our yeast two-hybrid assays revealed that ONAC103S exhibits strong self-interacting capability, and this activity is even more pronounced than that of the full-length ONAC103L. Since both

ONAC103L and ONAC103S have the same TRD, the enhanced interaction is potentially attributable to its N-terminal 18-amino-acid motif. Moreover, the ONAC103S–ONAC103L interaction is stronger than the homotypic ONAC103L–ONAC103L interaction (Figs. 9A, 9B). Based on these findings, we postulate that ONAC103S may competitively bind to ONAC103L, thereby interfering with its DNA-binding activity and attenuating its transcriptional function (Fig. 9C-G and Supplemental Fig. S7).

ONAC103L regulates rice leaf senescence by directly activating SAGs including *OsPAO*, *OsNOL*, *OsNAP* and *OsNYC4*. Among them, *OsNOL* and *OsPAO* are key chlorophyll catabolic genes in rice (Lee and Masclaux-Daubresse. 2021); *OsNAP* encodes a NAC transcription factor that regulates rice leaf senescence through an ABA-dependent pathway (Liang et al. 2014); and *OsNYC4* functions in degrading chlorophyll-protein complexes (Yamatani et al. 2013). All mutants of these genes exhibit stay-green phenotypes. Since both *ONAC103* and *OsNAP* are upregulated by ABA and involved in ABA-induced leaf senescence (Liang et al. 2014; Sun et al. 2024), we conclude that during the initiation of leaf senescence, increased ABA levels induce *ONAC103L*, which forms homodimers to activate the expression of genes associated with chlorophyll catabolism and chlorophyll-protein complex decomposition. In the later stages of leaf senescence, ONAC103S is highly expressed and interacts with ONAC103L, thereby disrupting its homodimerization and transcriptional activation activity, and contributing to the termination of the leaf senescence process mediated by ONAC103L (Fig. 10).

Conclusion

In summary, we found that the gene locus of ONAC103 generates two RNA isoforms through alternative promoter usage. The full-length isoform ONAC103L positively regulates rice leaf senescence via activating the target genes *OsPAO*, *OsNOL*, *OsNAP*, and *OsNYC4*; in contrast, the shorter isoform ONAC103S is N-terminally truncated and upregulated during the late stages of leaf senescence. It forms a heterodimer with ONAC103L, thereby impairing the ability of ONAC103L to activate its target genes and negatively regulating rice leaf senescence.

Materials and methods

Plant materials and growth conditions

All rice seeds used in this study were of the Oryza sativa L. cv. Zhonghua 11 (ZH11) background.

Overexpression transgenic lines were generated by cloning the genomic or cDNA fragments of *ONAC103L* and *ONAC103S*, respectively, into the pCAMBIA1306-3*Flag vector and introducing them into ZH11 via Agrobacterium-mediated transformation. Knockout mutants of *ONAC103* were generated using CRISPR-Cas9 technology, following the previously described protocols (Miao et al. 2013; Xie and Yang. 2013). Rice transformation was carried out by Boyuan Biotechnology Co., Ltd (Wuhan, China). Mutants and overexpression transgenic rice plants were identified by RT-qPCR using the primers listed in Supporting Information Table S1, or western blot against anti-FLAG monoclonal antibody (Proteintech,

USA). Seedlings were cultivated in growth chambers under a 12 h light (28°C) / 12 h dark (23°C) cycle. For phenotypic observation at the ripening stage and seed propagation, rice plants were grown in paddy fields in Taichang, Jiangsu Province (31°33'40"N, 121°09'18"E) from June to September, and in Sanya, Hainan Province (18°37'27"N, 109°48'28"E) from December to April in China.

Detection of gene expression level

Total RNA from plant tissues was extracted using TRIzol reagent (TaKaRa, Japan) and reverse transcribed into cDNA with the PrimeScript RT-PCR Kit containing a gDNA eraser (TaKaRa, Japan). RT-qPCR was carried out with 2× SYBR Green Master Mix (YEASEN, China). *OsUBQ5* was used as the internal reference gene, and gene expression levels were quantified using the 2^(-ΔΔCt) method. Primers for RT-qPCR are listed in Supporting Information Table S1.

Tobacco transient expression and Western blot

Nicotiana benthamiana were grown under 16 h/8 h light/dark (25°C, 60% relative humidity) for four weeks. The genomic fragment of *ONAC103*, as well as the cDNA fragments of *ONAC103L* and *ONAC103S*, were each cloned into the pCAMBIA1306-3*Flag vector and introduced into the *Agrobacterium* strain GV3101. The agrobacteria suspensions were infiltrated into the abaxial surface of tobacco leaves using a needleless syringe. Leaf samples were collected three to five days post-infiltration. Total proteins were extracted from the leaves and analyzed by western blot with an anti-FLAG monoclonal antibody (Proteintech, USA). The blot with the anti-actin antibody (Sangon Biotech Co., Ltd., Shanghai, China) was used as a loading control.

5’-RACE

Total RNA was isolated from rice leaves dark-induced for 5 days using the TaKaRa MiniBEST Plant RNA Extraction Kit (TaKaRa, Japan). The 5’-RACE assay was performed using the 5'-RACE Kit (Sangon Biotech Co., Ltd., China) following the manufacturer’s instructions.

GUS Staining Assay

The promoter sequences of *ONAC103L* and *ONAC103S* were cloned into a modified pCAMBIA1300 vector (Yao et al. 2018), respectively. The recombinant plasmids were transformed into *Agrobacterium tumefaciens* GV3101, and the resulting *Agrobacterium* suspensions were infiltrated into *Nicotiana benthamiana* leaves. Three days post-infiltration, the tobacco leaves were harvested for GUS staining using buffer composed of 10 mM EDTA (pH 8.0), 2 mM $K_4Fe(CN)_6$; 2 mM $K_3Fe(CN)_6$; 100 mM PBS (pH 7.0), 0.1%Triton-X-100, and 1 mg/ml X-Gluc.

Chlorophyll and ion leakage determination

Approximately 20–35 mg of rice leaves was ground into a fine powder, and chlorophyll was extracted following the method described previously (Porra et al. 1989). Chlorophyll contents (chlorophyll a, chlorophyll b, and total chlorophyll) were calculated using the following equations: Chlorophyll a = $(12.72A_{663} – 2.59A_{645}) \times V/(FW \times 1000)$, Chlorophyll b = $(22.88A_{645} – 4.67A_{663}) \times V/(FW \times 1000)$, and total chlorophyll = $(20.29A_{645} + 8.05A_{663}) \times V/(FW \times 1000)$. FW denotes the fresh weight of the leaf sample, and V refers to the volume of the extraction buffer. Ion leakage was measured following the method reported previously (Sakuraba et al. 2020).

Transcriptional activation and β-galactosidase activity assay

The coding regions of *ONAC103L* and *ONAC103S* were cloned into the pGBKT7 vector, respectively, and then transformed into competent yeast strain Y2HGold for transcriptional activation assay. Transformed cells were first selected on synthetic dropout (SD) medium lacking tryptophan (SD/-Trp), followed by spotting onto SD/-Trp-His-Ade medium for further validation. Genes with transcriptional activation activity are capable of growing on this triple dropout medium and turning blue in the presence of X-α-Gal. For the yeast two hybrid assay, genes predicted to interact were cloned into the pGADT7 and pGBKT7 vectors (Invitrogen, USA), respectively, and co-transformed into competent Y2HGold yeast cells. Positive clones were initially screened on SD/-Trp-Leu medium and subsequently spotted onto quadruple dropout medium (SD/-Trp-Leu-His-Ade) to verify potential protein-protein interactions. Activation of the reporter gene lacZ in yeast-based assays are quantified by determining the enzymatic activity of β-galactosidase using ortho-nitrophenyl-β-galactopyranoside (ONPG) as the substrate, as described previously (Möckli and Auerbach. 2004).

Preparation and transformation of rice protoplasts

Approximately two grams of fresh rice leaf sheaths harvested from 10-day-old seedlings were cut into small segments for protoplast isolation based on the methods described previously (Panda et al. 2024; Zhang et al. 2011). Subsequently, the plasmids were introduced into the isolated protoplasts following the PEG-mediated transformation protocol (Zhang et al. 2011).

Dual luciferase reporter assay

The coding sequences of *ONAC103L* and *ONAC103S* were cloned into the pCAMBIA1306 vector, respectively. Meanwhile, the promoter sequence of ONAC103L's target gene was inserted into the pGreenII-0800-LUC vector. The Dual-Luciferase Reporter Assay System (Promega, USA) was employed this assay following the manufacturer's instructions. After measuring the luminescence intensities of firefly luciferase (LUC) and Renilla luciferase (REN), the LUC/REN ratio was calculated to reflect the relative transcriptional activation activities of ONAC103L, ONAC103S, and ONAC103L plus ONAC103S toward the target genes.

Chromatin immunoprecipitation (ChIP)-qPCR assays

Two-week-old *ONAC103L-eYFP* overexpression transgenic seedlings were used for ChIP-qPCR as previously described (Yao et al. 2018). Immunoglobulin G (IgG) served as the negative control for the anti-GFP antibody (Proteintech, USA) and was subjected to identical experimental procedures throughout the ChIP assay. DNA was immunoprecipitated with the anti-GFP antibody and IgG, respectively, followed by further pull-down using protein A/G magnetic beads (Yeasen, China). After being cleaned and de-crosslinked, the purified DNA was used as the template for qPCR with primers designed against different regions of the target gene promoter. The ratio of DNA fragment enrichment (anti-GFP/IgG) was defined as the relative enrichment level. All primers used for ChIP-qPCR are provided in Supporting Information Table S1.

Electrophoretic mobility shift assay (EMSA)

The full-length CDS of *ONAC103L* and *ONAC103S* were cloned into the pMAL-c5G vector, respectively, and then transformed into Rosetta (DE3) competent cells for recombinant protein expression. The MBP-tagged recombinant proteins were purified with dextrin beads (Smart-Life Sciences, Changzhou, China) according to the manufacturer's protocol. Electrophoretic mobility shift assays (EMSAs) were carried out using the LightShift™ EMSA Optimization & Control Kit along with the Chemiluminescent Nucleic Acid Detection Module (Thermo Scientific, Waltham, MA, USA), following the manufacturer's instructions. 5'-biotin-labeled oligonucleotide probes (sequences are provided in Supporting Information Table S1) were synthesized and employed for EMSAs.

Gene accession numbers

Sequence data from this article can be found in the Rice Annotation Project Database (https://rapdb.dna.affrc.go.jp/) under the following accession numbers: *ONAC103* (LOC_Os07g48450), *OsNYC1* (LOC_Os01g12710), *OsNYC3* (LOC_Os06g24730), *OsNYC4* (LOC_Os07g37250), *OsNOL* (LOC_Os03g45194), *OsPAO* (LOC_Os03g05310), *OsNAC5* (LOC_Os11g08210), *OsNAC42* (LOC_Os09g32040) and *OsNAP* (LOC_Os03g21060).

Abbreviations

ABA: abscisic acid; SAGs: senescence-associated genes; CCGs: chlorophyll catabolic genes; TFs: transcription factors; TRD: transcriptional regulatory domain; TMD: transmembrane domain; ER: endoplasmic reticulum; sen-NAC: senescence-associated NAC; TSS: transcription start site; NLS□nuclear localization signal; NES: nuclear export signal; ChIP: chromatin immunoprecipitation; EMSA: electrophoretic mobility shift assay; DAP-Seq: DNA affinity purification sequencing; NACBS: NAC binding site; Y2H: yeast two-hybrid; SD: synthetic dropout; RACE: rapid amplification of cDNA ends; LUC: luciferase; REN: renilla luciferase; MeJA: methyl jasmonic acid; SA: salicylic acid; GA_3: gibberellic acid 3; IAA: indole-3-acetic acid; MRE: metal-responsive element; Ile: isoleucine; Thr: threonine; ZH11: zhonghua 11; ONPG: ortho-nitrophenyl-β-galactopyranoside.

Declarations

Ethics approval and consent to participate

Not applicable.

Consent for publication

All authors are consent for publication.

Availability of data and materials

No datasets were generated or analyzed during the current study. All data supporting the conclusions of this article are provided in the article and its supplementary information files.

Competing interests

The authors declare that they have no competing interests.

Funding

This research was supported by the National Natural Science Foundation of China (No.32570334 and No.31970343) and Shanghai Natural Science Foundation (No. 23ZR1403400) to X.G.

Authors' contributions

X.G. and S.A. designed the research; S.A., Y.H. and X.C. performed the experiments and analyzed the data; S.A. and X.G. wrote the manuscript, and X.G. revised the manuscript.

Acknowledgments

We are grateful to Professors Xiaojin Luo and Zhiping Song at Fudan University for their generous provision of the field plots for rice growth.

References

1. Bachmair A, Varshavsky A (1989) The degradation signal in a short-lived protein. Cell 56(6): 1019-1032.
2. Balazadeh S, Kwasniewski M, Caldana C, Mehrnia M, Zanor MI, Xue GP, Mueller-Roeber B (2011) ORS1, an H_2O_2-responsive NAC transcription factor, controls senescence in Arabidopsis thaliana. Molecular Plant 4(2): 346-360.
3. Balazadeh S, Siddiqui H, Allu AD, Matallana-Ramirez LP, Caldana C, Mehrnia M, Zanor MI, Köhler B, Mueller-Roeber B (2010) A gene regulatory network controlled by the NAC transcription factor ANAC092/AtNAC2/ORE1 during salt-promoted senescence. Plant Journal 62(2): 250-264.
4. Davuluri RV, Suzuki Y, Sugano S, Plass C, Huang THM (2008) The functional consequences of alternative promoter use in mammalian genomes. Trends in Genetics 24(4): 167-177.

5. de Klerk E, 't Hoen PAC (2015) Alternative mRNA transcription, processing, and translation: insights from RNA sequencing. Trends in Genetics 31(3): 128-139.
6. El Mannai Y, Akabane K, Hiratsu K, Satoh-Nagasawa N, Wabiko H (2017) The NAC transcription factor gene (*ONAC011*) promotes leaf senescence and accelerates heading time in rice. International Journal of Molecular Sciences 18(10).
7. Fang YJ, You J, Xie KB, Xie WB, Xiong LZ (2008) Systematic sequence analysis and identification of tissue-specific or stress-responsive genes of NAC transcription factor family in rice. Molecular Genetics and Genomics 280(6): 547-563.
8. Gao S, Gao J, Zhu XY, Song Y, Li ZP, Ren GD, Zhou X, Kuai BK (2016) ABF2, ABF3, and ABF4 promote ABA-mediated chlorophyll degradation and leaf senescence by transcriptional activation of chlorophyll catabolic genes and senescence-associated genes in *Arabidopsis*. Molecular Plant 9(9): 1272-1285.
9. Guo YF, Gan SS (2006) AtNAP, a NAC family transcription factor, has an important role in leaf senescence. Plant Journal 46(4): 601-612.
10. Guo YF, Ren GD, Zhang KW, Li ZH, Miao Y, Guo HW (2021) Leaf senescence: progression, regulation, and application. Molecular Horticulture 1(1).
11. Hernández G, Osnaya VG, Pérez-Martínez X (2019) Conservation and variability of the AUG initiation codon context in eukaryotes. Trends in Biochemical Sciences 44(12): 1009-1021.
12. Hu HH, Dai MQ, Yao JL, Xiao BZ, Li XH, Zhang QF, Xiong LZ (2006) Overexpressing a NAM, ATAF, and CUC (NAC) transcription factor enhances drought resistance and salt tolerance in rice. Proceedings of the National Academy of Sciences of the United States of America 103(35): 12987-12992.
13. Jensen MK, Kjaersgaard T, Nielsen MM, Galberg P, Petersen K, O'Shea C, Skriver K (2010) The NAC transcription factor family: structure-function relationships and determinants of ANAC019 stress signalling. Biochemical Journal 426: 183-196.
14. Kang K, Shim Y, Gi E, An G, Paek NC (2019) Mutation of *ONAC096* enhances grain yield by increasing panicle number and delaying Leaf senescence during grain filling in rice. International Journal of Molecular Sciences 20(20).
15. Kim HJ, Park JH, Kim J, Kim JJ, Hong S, Kim J, Kim JH, Woo HR, Hyeon C, Lim PO, Nam HG, Hwang D (2018) Time- evolving genetic networks reveal a NAC troika that negatively regulates leaf senescence in *Arabidopsis*. Proceedings of the National Academy of Sciences of the United States of America 115(21): E4930-E4939.
16. Kjaersgaard T, Jensen MK, Christiansen MW, Gregersen P, Kragelund BB, Skriver K (2011) Senescence-associated barley NAC (NAM, ATAF1,2, CUC) transcription factor interacts with radical-induced Cell Death 1 through a disordered regulatory domain. Journal of Biological Chemistry 286(41): 35418-35429.
17. Kozak M (1987) An analysis of 5'-noncoding sequences from 699 vertebrate messenger-rnas. Nucleic Acids Research 15(20): 8125-8148.

18. Lee S, Masclaux-Daubresse C (2021) Current understanding of leaf senescence in rice. International Journal of Molecular Sciences 22(9).
19. Li LJ, He Y, Zhang ZH, Shi YF, Zhang XB, Xu X, Wu JL, Tang SQ (2021) OsNAC109 regulates senescence, growth and development by altering the expression of senescence- and phytohormone-associated genes in rice. Plant Molecular Biology 105(6): 637-654.
20. Liang CZ, Wang YQ, Zhu YN, Tang JY, Hu B, Liu LC, Ou SJ, Wu HK, Sun XH, Chu JF, Chu CC (2014) OsNAP connects abscisic acid and leaf senescence by fine-tuning abscisic acid biosynthesis and directly targeting senescence-associated genes in rice. Proceedings of the National Academy of Sciences of the United States of America 111(27): 10013-10018.
21. Lim PO, Kim HJ, Nam HG (2007) Leaf senescence. Annual Review of Plant Biology 58: 115-136.
22. Liu Q, Liu W, Niu Y, Wang T, Dong J (2024) Liquid–liquid phase separation in plants: Advances and perspectives from model species to crops. Plant Communications 5(1).
23. Mao CJ, Lu SC, Lv B, Zhang B, Shen JB, He JM, Luo LQ, Xi DD, Chen X, Ming F (2017) A rice NAC transcription factor promotes leaf senescence via ABA biosynthesis. Plant Physiology 174(3): 1747-1763.
24. Mathew IE, Agarwal P (2018) May the fittest protein evolve: favoring the plant-specific origin and expansion of NAC transcription factors. Bioessays 40(8).
25. Miao J, Guo DS, Zhang JZ, Huang QP, Qin GJ, Zhang X, Wan JM, Gu HY, Qu LJ (2013) Targeted mutagenesis in rice using CRISPR-Cas system. Cell Research 23(10): 1233-1236.
26. Möckli N, Auerbach D (2004) Quantitative β-galactosidase assay suitable for high-throughput applications in the yeast two-hybrid system. Biotechniques 36(5): 872-876.
27. Nagahage ISP, Matsuda K, Miyashita K, Fujiwara S, Mannapperuma C, Yamada T, Sakamoto S, Ishikawa T, Nagano M, Ohtani M, Kato K, Uchimiya H, Mitsuda N, Kawai-Yamada M, Demura T, Yamaguchi M (2023) NAC domain transcription factors VNI2 and ATAF2 form protein complexes and regulate leaf senescence. Plant Direct 7(9).
28. Nuruzzaman M, Manimekalai R, Sharoni AM, Satoh K, Kondoh H, Ooka H, Kikuchi S (2010) Genome-wide analysis of NAC transcription factor family in rice. Gene 465(1-2): 30-44.
29. O'Shea C, Kryger M, Stender EGP, Kragelund BB, Willemoës M, Skriver K (2015) Protein intrinsic disorder in NAC transcription factors: transcriptional activation by ANAC013 and ANAC046 and their interactions with RCD1. Biochemical Journal 465: 281-294.
30. Olsen AN, Ernst HA, Lo Leggio L, Skriver K (2005) NAC transcription factors: structurally distinct, functionally diverse. Trends in Plant Science 10(2): 79-87.
31. Panda D, Karmakar S, Dash M, Tripathy SK, Das P, Banerjee S, Qi YP, Samantaray S, Mohapatra PK, Baig MJ, Molla KA (2024) Optimized protoplast isolation and transfection with a breakpoint: accelerating Cas9/sgRNA cleavage efficiency validation in monocot and dicot. Abiotech 5(2): 151-168.
32. Porra RJ, Thompson WA, Kriedemann PE (1989) Determination of accurate extinction coefficients and simultaneous-equations for assaying chlorophyll-a and chlorophyll-b extracted with 4 different

solvents - verification of the concentration of chlorophyll standards by atomic-absorption spectroscopy. Biochimica Et Biophysica Acta 975(3): 384-394.

33. Puranik S, Sahu PP, Srivastava PS, Prasad M (2012) NAC proteins: regulation and role in stress tolerance. Trends in Plant Science 17(6): 369-381.
34. Qi XT, Zhang YX, Chai TY (2007) The bean gene produces two transcripts by alternative promoter usage. Biochemical and Biophysical Research Communications 356(1): 273-278.
35. Sakuraba Y, Kim D, Han SH, Kim SH, Piao W, Yanagisawa S, An G, Paek NC (2020) Multilayered regulation of membrane-bound ONAC054 is essential for abscisic acid-induced leaf senescence in rice. Plant Cell 32(3): 630-649.
36. Sakuraba Y, Piao W, Lim JH, Han SH, Kim YS, An G, Paek NC (2015) Rice ONAC106 inhibits leaf senescence and increases salt tolerance and tiller angle. Plant and Cell Physiology 56(12): 2325-2339.
37. Sriram SM, Kim BY, Kwon YT (2011) The N-end rule pathway: emerging functions and molecular principles of substrate recognition. Nature Reviews Molecular Cell Biology 12(11): 735-747.
38. Sun L, Xu HQ, Song J, Yang XY, Wang XY, Liu HY, Pang MZ, Hu YC, Yang Q, Ning XT, Liang SS, Zhang SJ, Luan WJ (2024) OsNAC103, a NAC transcription factor, positively regulates leaf senescence and plant architecture in rice. Rice 17(1).
39. Tran LSP, Nakashima K, Sakuma Y, Simpson SD, Fujita Y, Maruyama K, Fujita M, Seki M, Shinozaki K, Yamaguchi-Shinozaki K (2004) Isolation and functional analysis of *Arabidopsis* stress-inducible NAC transcription factors that bind to a drought-responsive-element in the promoter. Plant Cell 16(9): 2481-2498.
40. Ushijima T, Hanada K, Gotoh E, Yamori W, Kodama Y, Tanaka H, Kusano M, Fukushima A, Tokizawa M, Yamamoto YY, Tada Y, Suzuki Y, Matsushita T (2017) Light controls protein localization through phytochrome-mediated alternative promoter selection. Cell 171(6): 1316-+.
41. Wang HL, Zhang Y, Wang T, Yang Q, Yang YL, Li Z, Li BS, Wen X, Li WY, Yin WL, Xia XL, Guo HW, Li ZH (2021) An alternative splicing variant of PtRD26 delays leaf senescence by regulating multiple NAC transcription factors in *Populus*. Plant Cell 33(5): 1594-1614.
42. Wang P, Li Y, Liu Z, Li XH, Wang YC, Liu WJ, Li X, Hu JJ, Zhu WY, Wang CQ, Li S, Gu TT, Xu DQ, Tang C, Wang YT, Li C, Zhang SL, Wu JY (2023) Reciprocal regulation of flower induction by ELF3α and ELF3β generated via alternative promoter usage. Plant Cell 35(6): 2095-2113.
43. Xie KB, Yang YN (2013) RNA-guided genome editing in plants using a CRISPRCas system. Molecular Plant 6(6): 1975-1983.
44. Xiong HY, He HD, Chang Y, Miao BB, Liu ZW, Wang QQ, Dong FM, Xiong LZ (2025) Multiple roles of NAC transcription factors in plant development and stress responses. Journal of Integrative Plant Biology 67(3): 510-538.
45. Yamaguchi M, Ohtani M, Mitsuda N, Kubo M, Ohme-Takagi M, Fukuda H, Demura T (2010) VND-INTERACTING2, a NAC domain transcription factor, negatively regulates xylem vessel formation in *Arabidopsis*. Plant Cell 22(4): 1249-1263.

46. Yamatani H, Sato Y, Masuda Y, Kato Y, Morita R, Fukunaga K, Nagamura Y, Nishimura M, Sakamoto W, Tanaka A, Kusaba M (2013) NYC4, the rice ortholog of *Arabidopsis* THF1, is involved in the degradation of chlorophyll protein complexes during leaf senescence. Plant Journal 74(4): 652-662.
47. Yao LY, Cheng X, Gu ZY, Huang W, Li S, Wang LB, Wang YF, Xu P, Ma H, Ge XC (2018) The AWPM-19 family protein OsPM1 mediates abscisic acid influx and drought response in rice. Plant Cell 30(6): 1258-1276.
48. Yu GH, Xie ZN, Lei SS, Li H, Xu B, Huang BR (2022) The NAC factor LpNAL delays leaf senescence by repressing two chlorophyll catabolic genes in perennial ryegrass. Plant Physiology 189(2): 595-610.
49. Zhang Y, Su JB, Duan S, Ao Y, Dai JR, Liu J, Wang P, Li YG, Liu B, Feng DR, Wang JF, Wang HB (2011) A highly efficient rice green tissue protoplast system for transient gene expression and studying light/chloroplast-related processes. Plant Methods 7.
50. Zhu XY, Chen JY, Xie ZK, Gao J, Ren GD, Gao S, Zhou X, Kuai BK (2015) Jasmonic acid promotes degreening via MYC2/3/4-and ANAC019/055/072-mediated regulation of major chlorophyll catabolic genes. Plant Journal 84(3): 597-610.

Figures

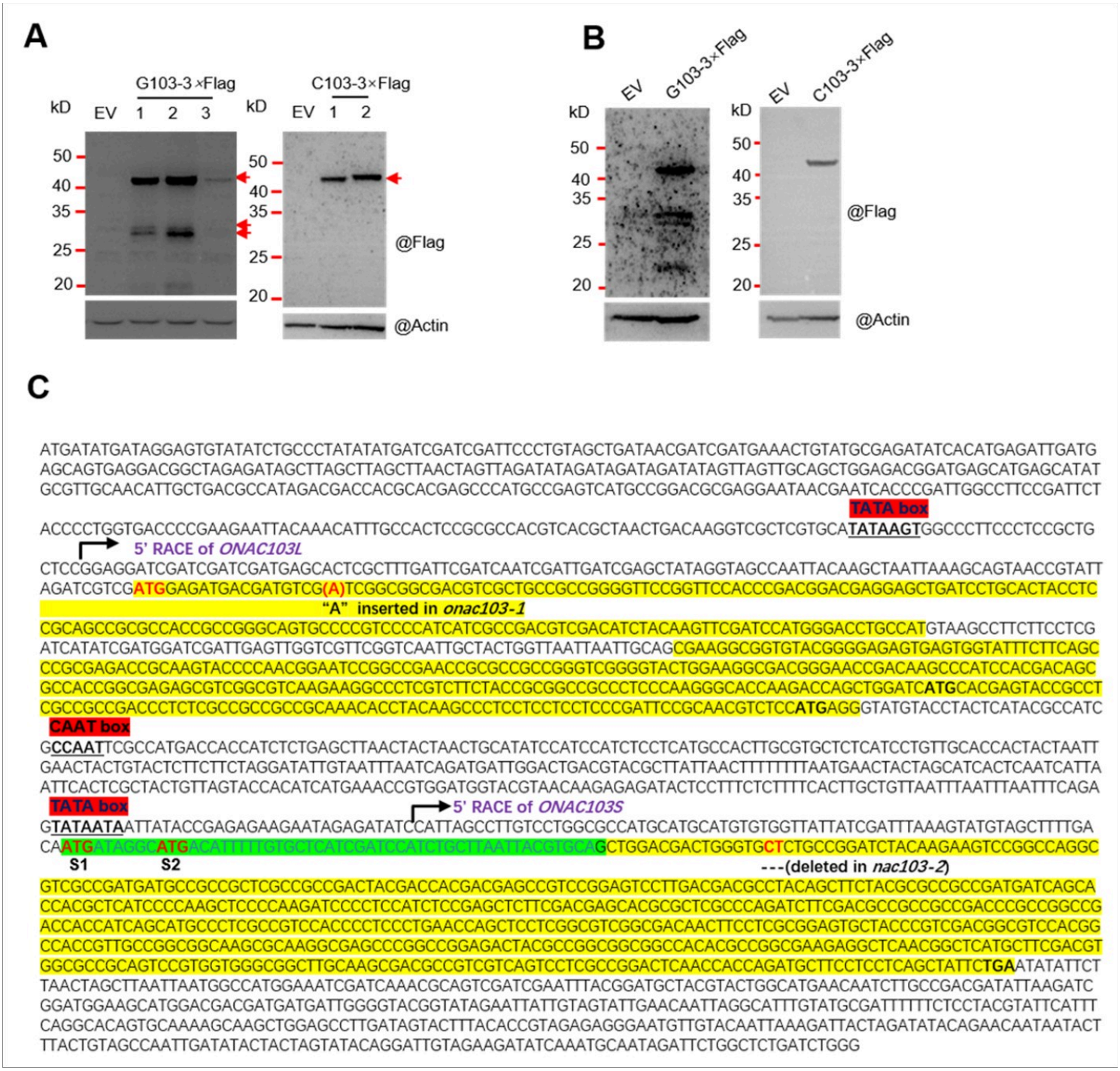


Figure 1

The *ONAC103* gene locus generates multiple isoforms. A. Western blot analysis of ONAC103 protein in *35S: G103-3×Flag and 35S: C103-3×Flag* transgenic plants. Leaves of transgenic lines were harvested for ONAC103 detection with protease inhibitor cocktail to inhibit cellular protease activity. B. The constructs of *35S: G103-3×Flag* and *35S: C103-3×Flag* were introduced into tobacco leaves for transient protein expression. ONAC103 proteins were detected using an anti-Flag antibody, with protease inhibitor cocktail to inhibit cellular protease activity. C. Genomic DNA sequence of the *ONAC103* gene locus. Sequences highlighted in yellow represent exons. The sequence highlighted in green is the coding sequence present in *ONAC103S* but absent in *ONAC103L*, which encodes the N-terminal 18 amino acids of ONAC103S.

Sequences downstream of the green-highlighted region are shared by both *ONAC103L* and *ONAC103S*. The transcription start site (TSS) of
NAC103L and *ONAC103S* determined by 5'-RACE are shown by arrows.

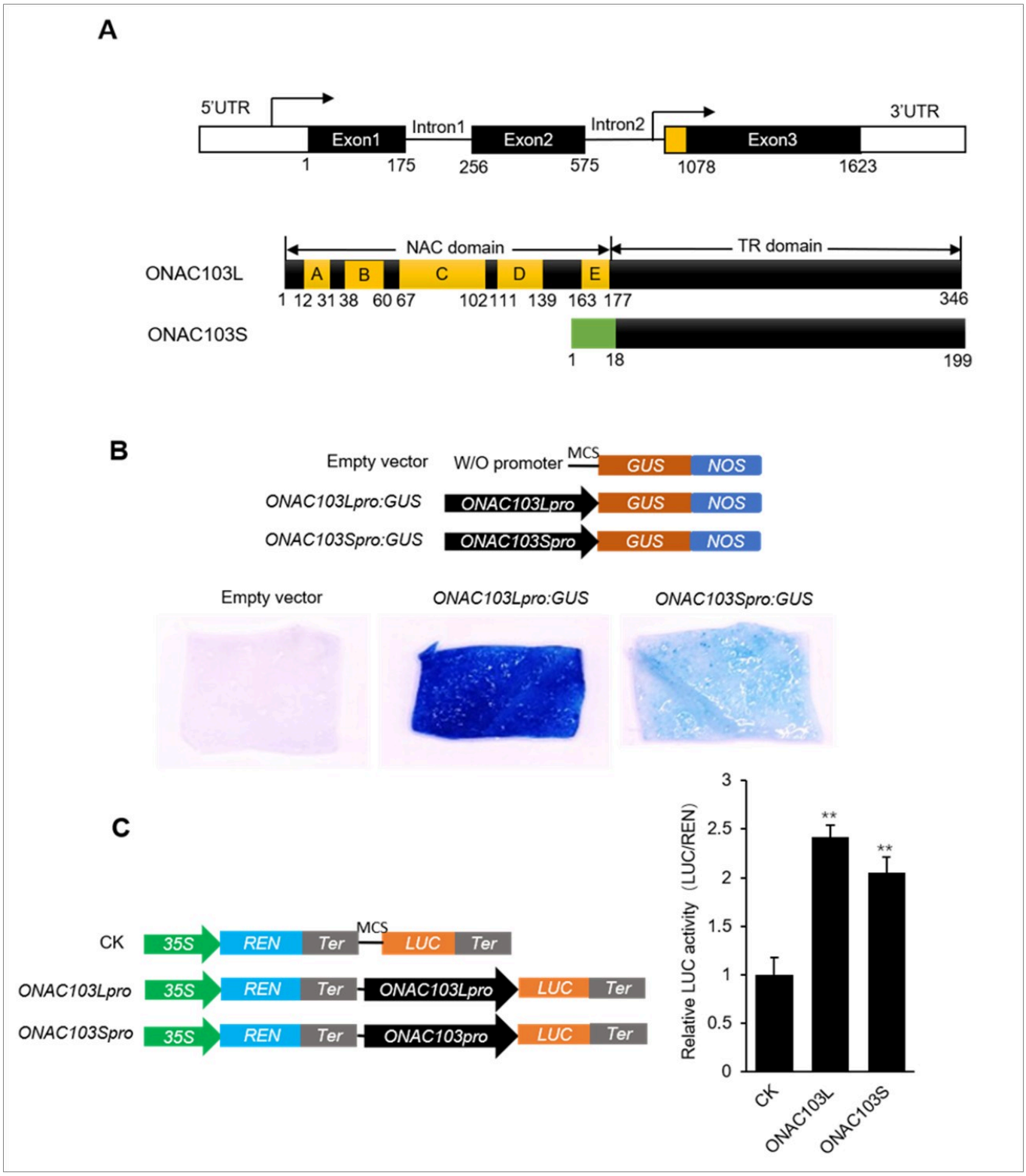


Figure 2

The intronic promoter of *ONAC103* gene locus is functional. A. Gene Structure of *ONAC103*gene locus and protein domain compositions of ONAC103L and ONAC103S. B. GUS reporter assay of the *ONAC103L* promoter and *ONAC103S* promoter activities in tobacco leaves. *ONAC103L* and *ONAC103S* promoters were fused with *GUS* gene and cloned into a modified pCAMBIA1300 vector. *Agrobacteria* carrying the recombinant plasmid and the empty vector were infiltrated into tobacco leaves for protein expression. C. Quantification of the promoter activity in rice protoplasts by dual luciferase assay.

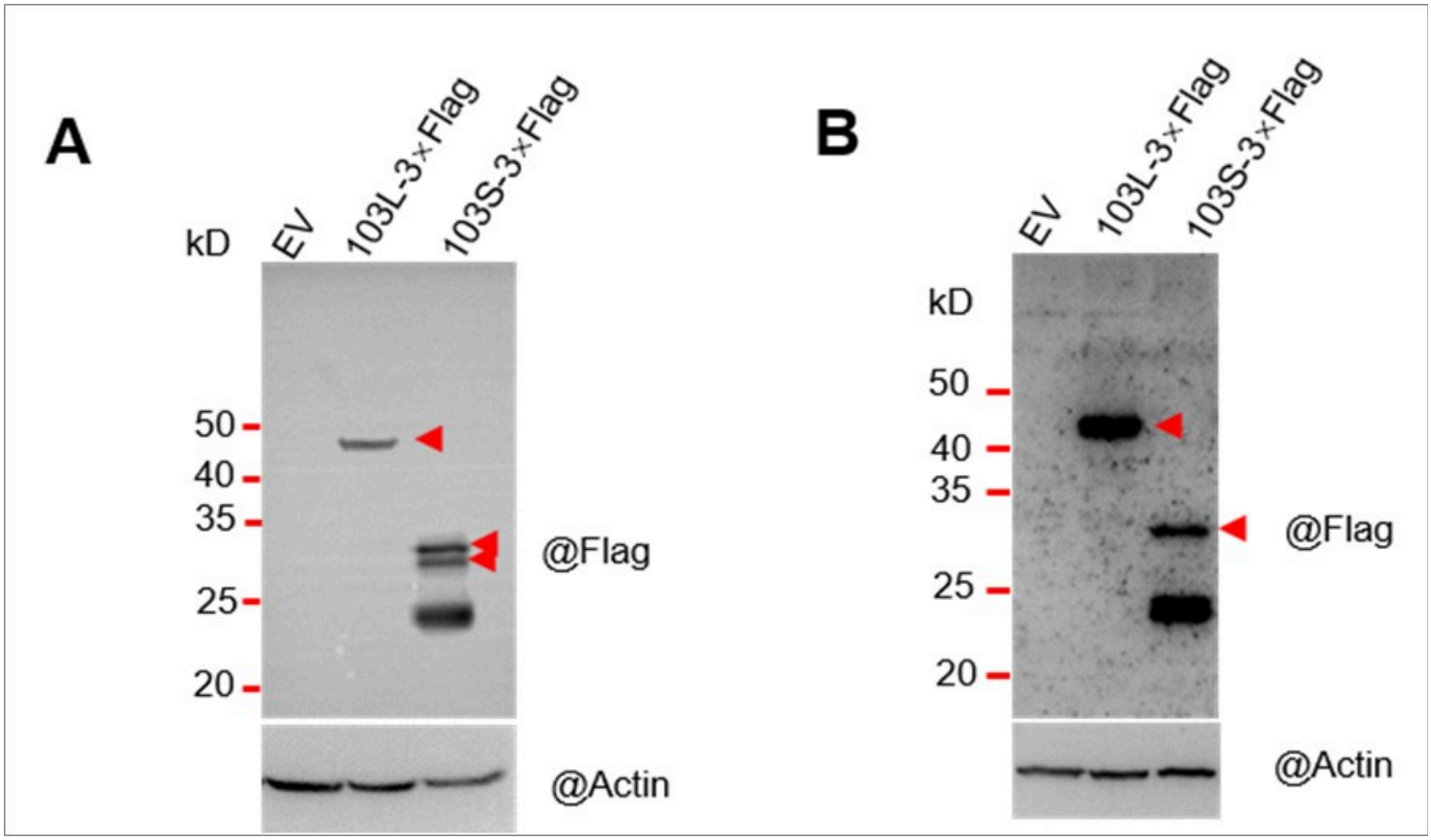


Figure 3

The *ONAC103S* RNA isoform generates protein bands matching the additional bands observed in genomic *ONAC103*transgenic lines. A. Detection of ONAC103 proteins in tobacco leaves transformed with *35S:103L-3×Flag* and *35S:103S-3×Flag* constructs, with the protease inhibitor cocktail to suppress the cellular protease activities. B. Detection of ONAC103 proteins in *35S: 103L-3×Flag* and *35S: 103S-3× Flag* transgenic rice plants. Leaves from positive transgenic lines were harvested for ONAC103 detection, with the protease inhibitor cocktail to suppress the cellular protease activities.

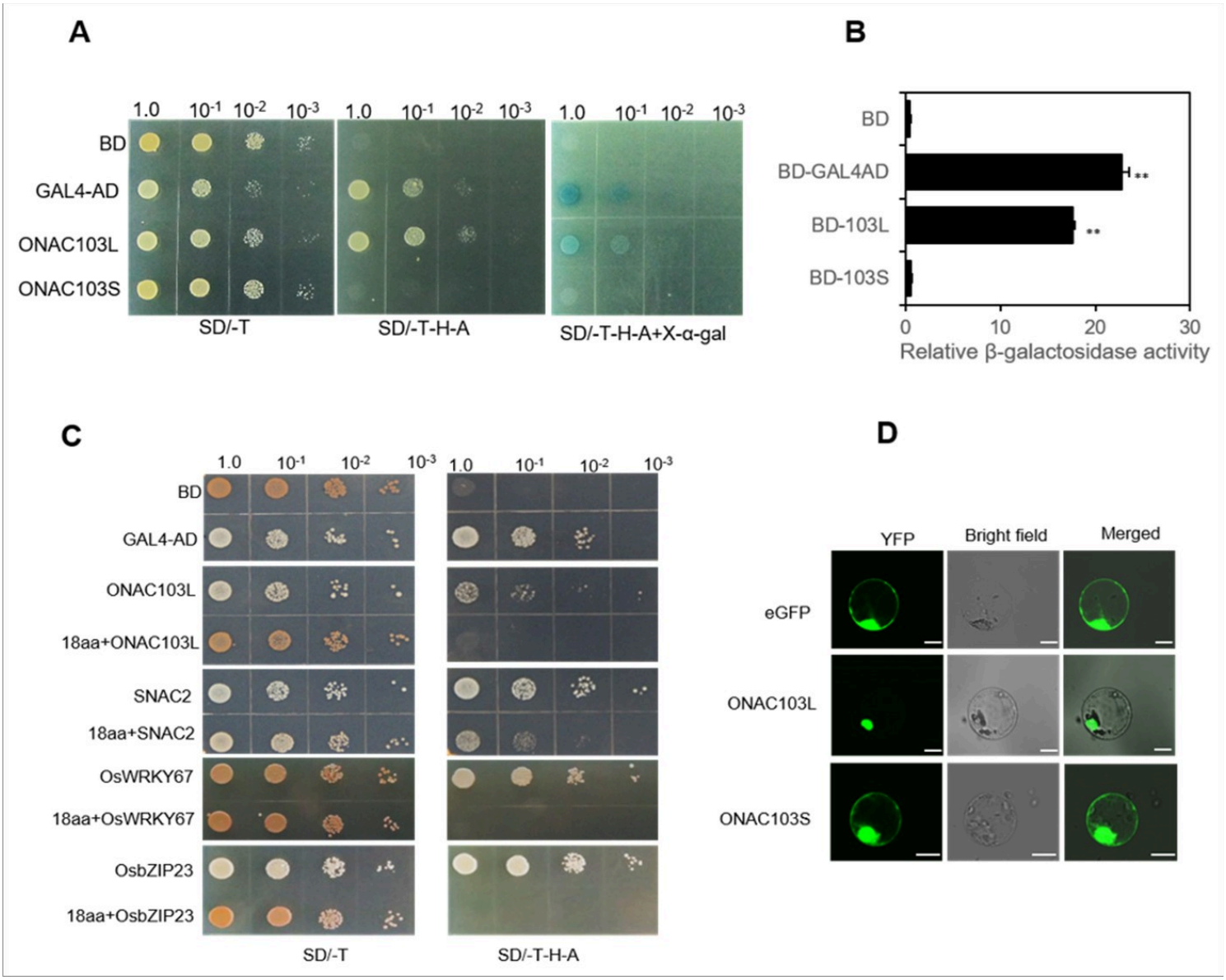


Figure 4

Transcriptional activation assay of ONAC103 isoforms. A. Transcriptional activation assay of ONAC103L and ONAC103S in yeast system using GAL4-AD as positive control (GAL4 activation domain is cloned into pGBKT7 vector) and BD (pGBKT7 empty vector) as negative control. SD: basic medium, T: tryptophan, H: histidine, A: adenine. B. Quantitative determination of the transcriptional activation activities of ONAC103L and ONAC103S by β-galactosidase activity assay. Data are means ± SD (n = 3). Error bar indicates standard deviation. Student's t-test: ** $P \leq 0.01$. C. Inhibitory effects of the 18 aa peptide on different transcription factors in yeast. D. Subcellular localization results of ONAC103L and ONAC103S in rice protoplasts. The *35S: eGFP*, *35S: eGFP-ONAC103L* and *35S: eGFP-ONAC103S* plasmids were transformed into rice protoplasts, respectively and the fluorescence signals were observed.

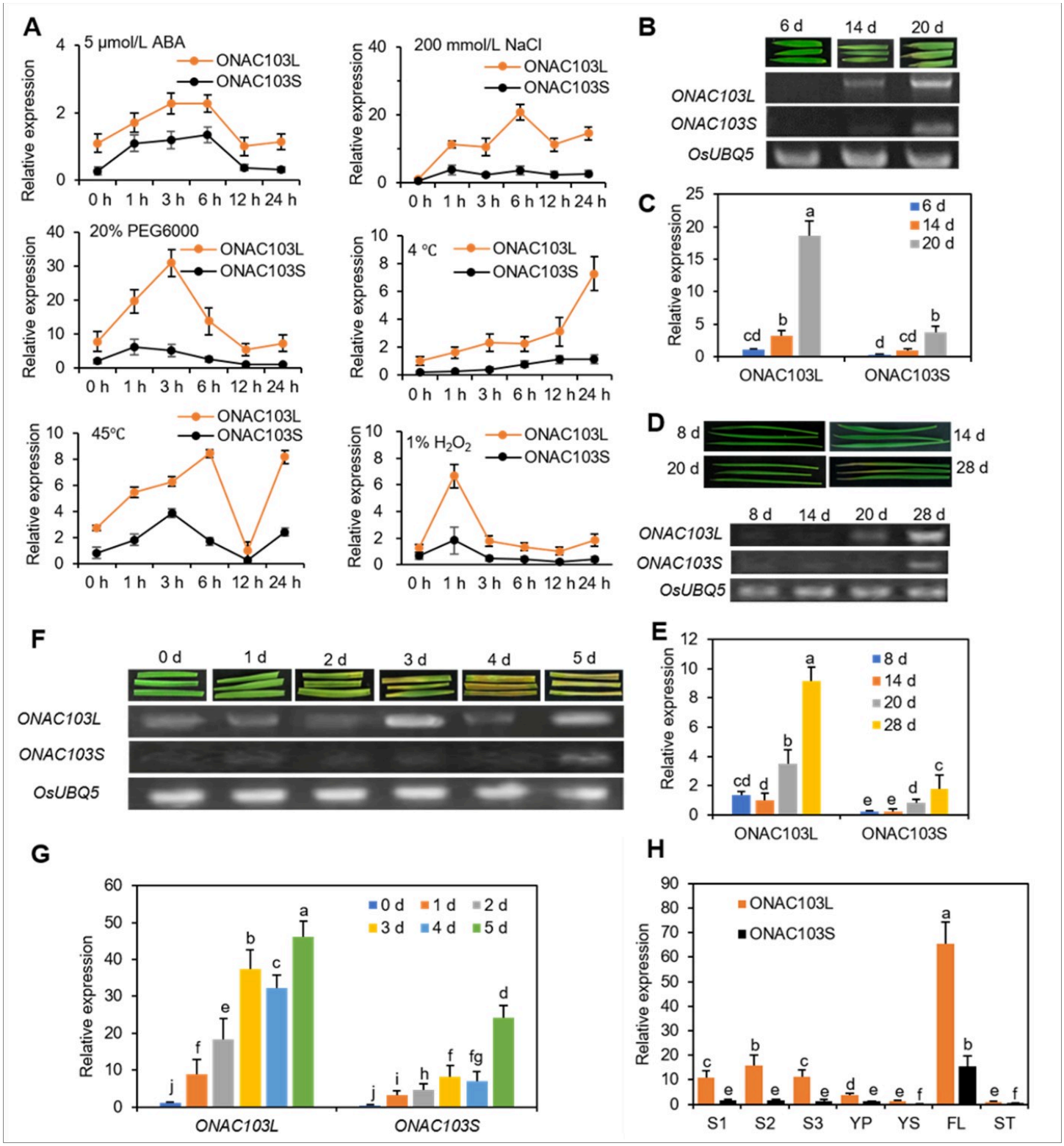


Figure 5

Expression patterns of *ONAC103L* and *ONAC103S*. Transcriptional changes of *ONAC103L*and *ONAC103S* in response to ABA treatment and various abiotic stresses. Eleven-day-old rice seedlings were treated with 5 μmol/L ABA, 200 mmol/L NaCl, 20% PEG6000, 4 °C, 45 °C, and 1% H_2O_2 for different time periods, respectively. Leaves were harvested to determine the expression levels of *ONAC103L* and *ONAC103S*via RT-qPCR. B-C. Transcriptional changes of *ONAC103L* and *ONAC103S*in the first leaf during natural

senescence. Semi-quantitative RT-PCR (B) and RT-qPCR (C) were used to detect the expression levels of *ONAC103L* and *ONAC103S* in the first leaf of ZH11 at 6, 14, and 20 days after germination. D-E. Transcriptional changes of *ONAC103L* and *ONAC103S* in the second leaf during natural senescence. Semi-quantitative RT-PCR (D) and RT-qPCR (E) were employed to measure the expression levels of *ONAC103L* and *ONAC103S*in the second leaf of ZH11 at 8, 14, 20, and 28 days after germination. F-G. Transcriptional changes of *ONAC103L* and *ONAC103S* in rice leaves under dark-induced senescence. The second leaf of 24-day-old ZH11 seedlings was subjected to dark induction for 5 days, and the expression levels of *ONAC103L*and *ONAC103S* were examined daily by semi-quantitative RT-PCR (F) and RT-qPCR (G). H. Expression patterns of *ONAC103L* and *ONAC103S* in various rice tissues. S1: Spikelet (3.0 mm~3.5 mm in length); S2: Spikelet (3.5 mm~4.0 mm in length); S3: Spikelet (4.0 mm~4.5 mm in length); YP: Young Panicle; YS: Young Stem; FL: Flag leaf; ST: Stem. Data are presented as means ± SD (n = 3). *OsUBQ5* was used as an internal control in all experiments. Two-way ANOVA was performed to determine statistical significance.

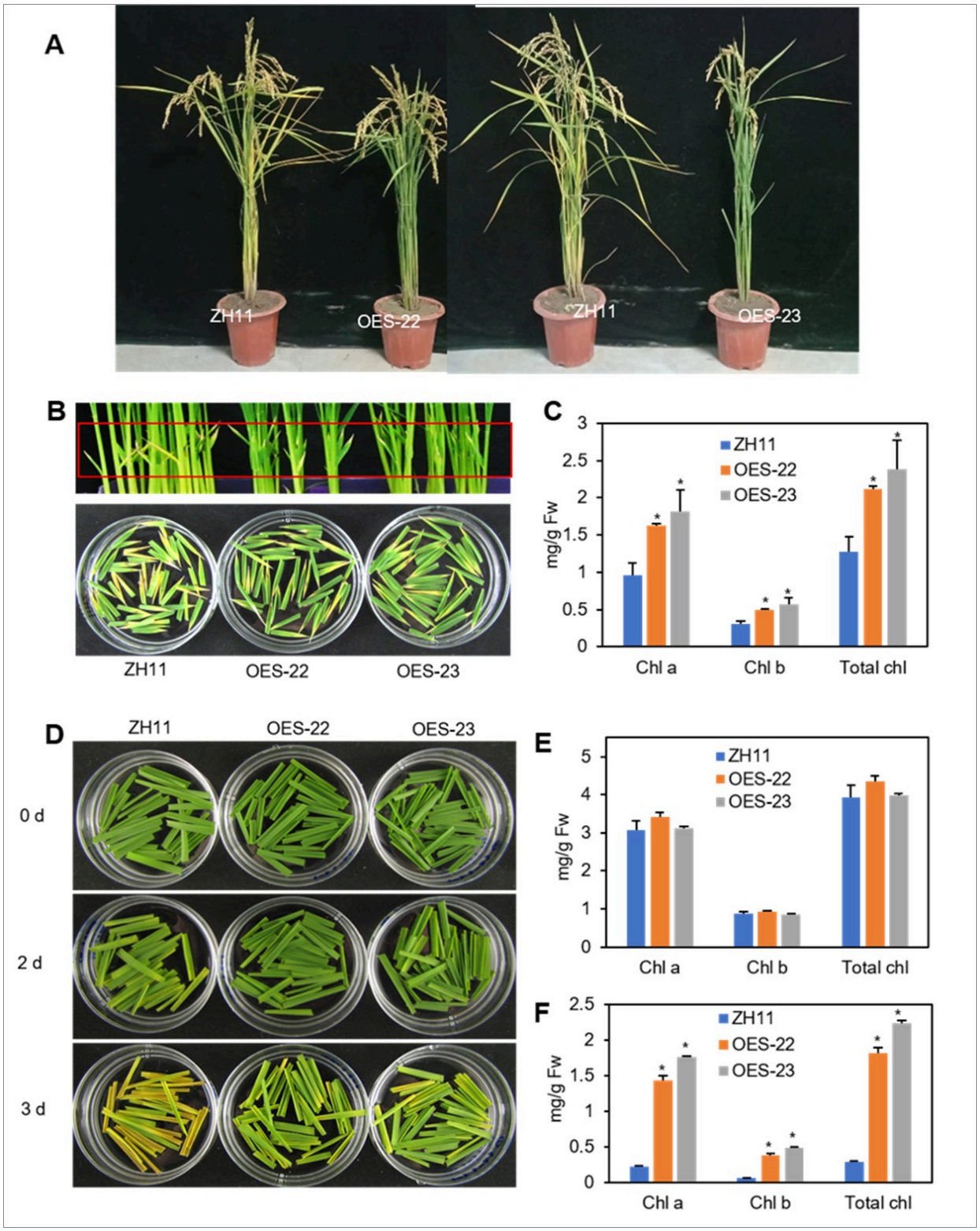


Figure 6

ONAC103S-overexpression lines exhibit a delayed senescence phenotype as *onac103* mutants. A. Leaf senescence of *ONAC103S*-overexpression lines was delayed compared to ZH11 at the ripening stage. B. Comparison of the first leaf color between ZH11 and *ONAC103S*-overexpression seedlings at 18 days after germination. The first leaves of each line are boxed (top panel), and detached leaves are shown in a group shot (bottom panel). C. Determination of chlorophyll content in the first leaves of each line at 18

days after germination. D. Dark-induced senescence phenotype of the second leaves from each line. The second leaves of 17-day-old seedlings were subjected to dark induction and photographed on day 0, day 2, and day 3. E-F. Chlorophyll content of the second leaves before (E) and after dark induction (F). The second leaves of 17-day-old seedlings were subjected to dark induction, with chlorophyll content measured at 0 day and 3 days after induction. Data are presented as means ± SD (n = 3). Statistical analysis was conducted using Student's t-test. * P ≤ 0.05; ** P ≤ 0.01.

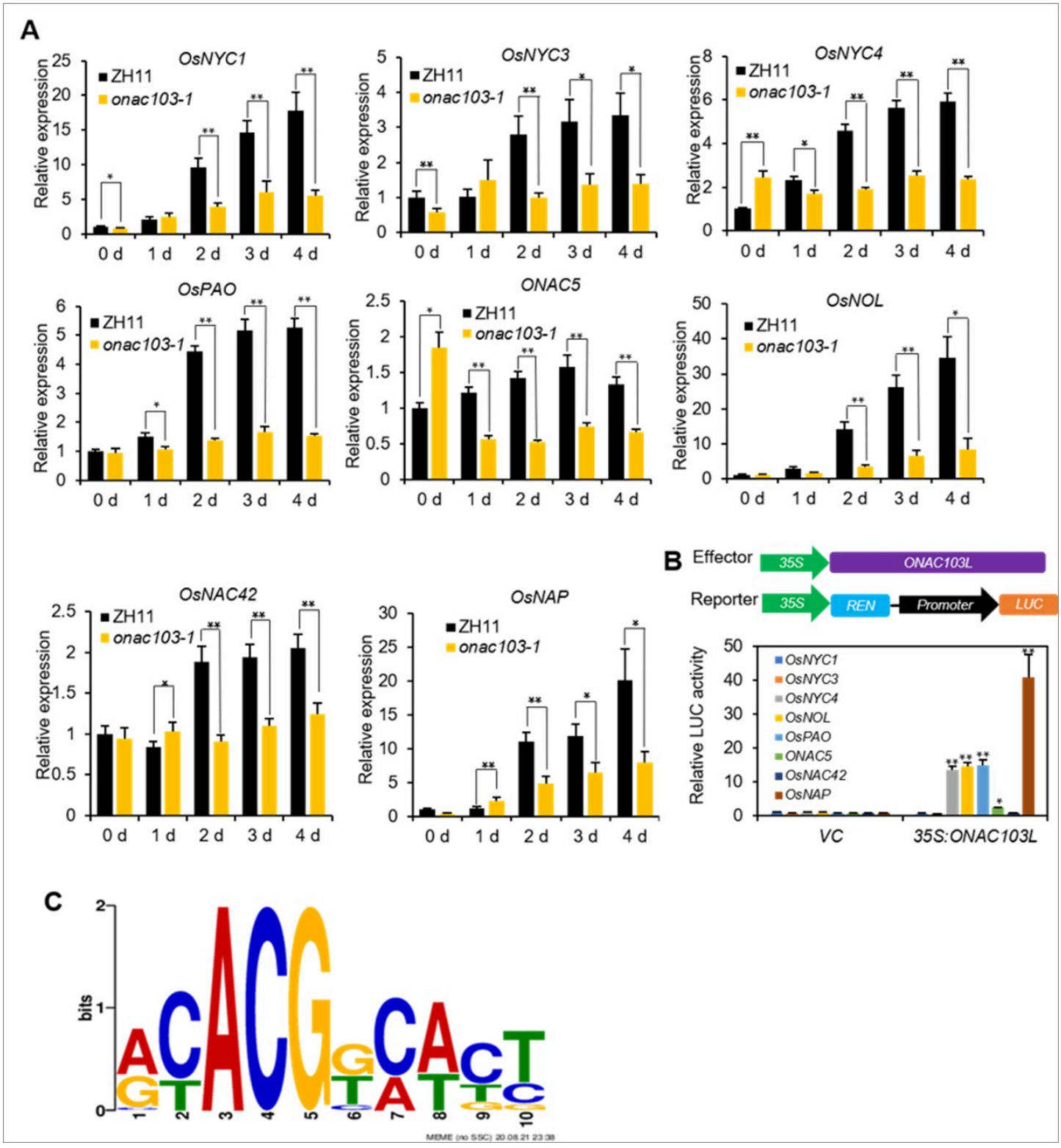


Figure 7

ONAC103L activates the expression of senescence-associated genes. A. Expression level comparison of senescence-associated genes between ZH11 and the *onac103-1*mutant. First leaves of one-week-old ZH11 and *onac103-1* seedlings were harvested and subjected to dark-induced senescence. Samples were collected daily after induction. B. Dual-luciferase reporter assay showed that ONAC103L activates the expression of senescence-associated genes in rice protoplasts. VC indicates the empty vector, with the LUC/REN ratio of VC set to 1. Data are presented as means ± SD (n = 3). Statistical analysis was conducted using Student's t-test. * $P \leq 0.05$; ** $P \leq 0.01$. C. DAP-Seq identified the DNA-binding motif of ONAC103L. The Position Weight Matrix (PWM) for each site is shown.

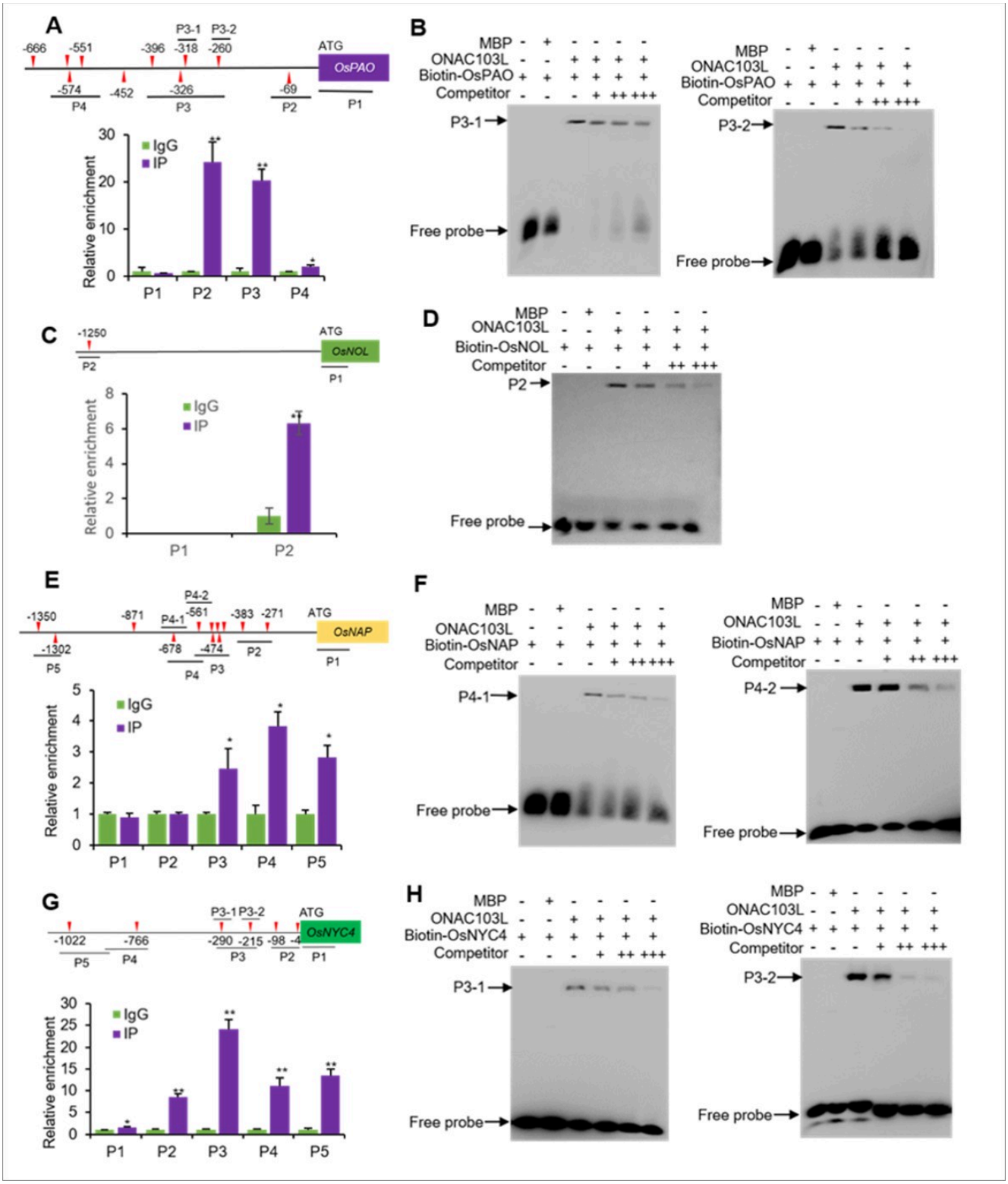


Figure 8

ChIP-qPCR and EMSA analyses demonstrate that ONAC103L directly binds to the promoters of multiple target genes. A, C, E, G. Enrichment of ONAC103L on the promoters of *OsPAO* (A), *OsNOL* (C), *OsNAP* (E), and *OsNYC4*(G). Schematic diagrams depicting the core motif (CACG) of ONAC103 binding sites and the amplified regions on the promoters are presented above the qPCR results. Red triangles indicate the predicted ONAC103L binding sites. The enrichment level of IgG was set to 1. Data are presented as

means ± SD (n = 3). Statistical analysis was conducted using Student's t-test. *, P ≤ 0.05; **, P ≤ 0.01. B, D, F, H. EMSA analysis verifying the binding of ONAC103L to the promoters of *OsPAO* (B), *OsNOL* (D), *OsNAP* (F), and *OsNYC4*(H). Purified MBP-ONAC103L fusion protein and MBP tag protein alone were used for EMSA assays. +, ++ and +++ indicate increasing concentrations of unlabeled competitor probe, respectively.

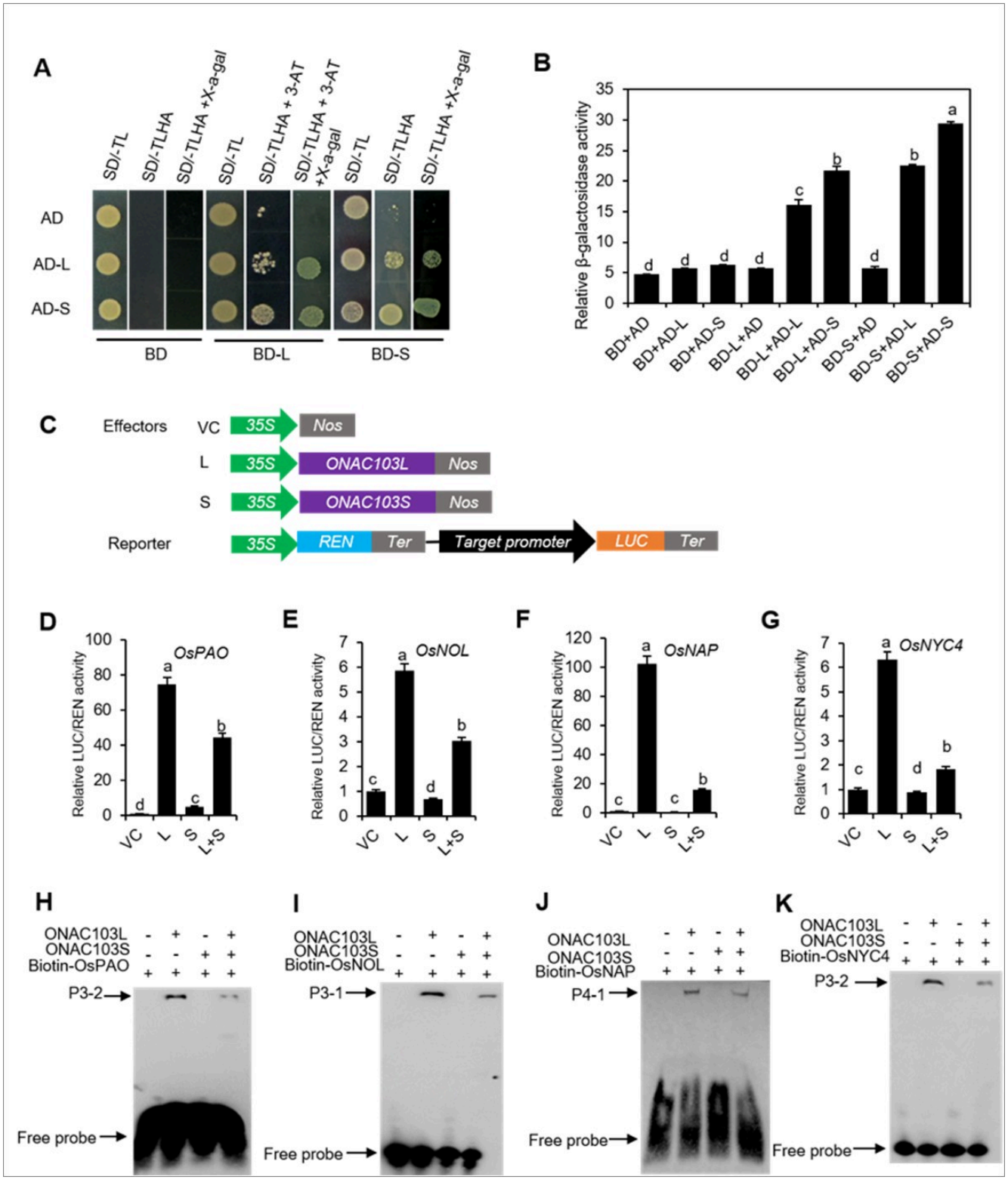


Figure 9

ONAC103S represses the transcriptional activation activity of ONAC103L. A.Yeast two-hybrid analysis showing that ONAC103L interacted with ONAC103S. The bait and prey pairs were co-transformed into yeast cells and selected on SD/-TL and SD/−TLHA media, respectively. 3-AT was used to suppress the self-activation of ONAC103L. L, ONAC103L; S, ONAC103S. B. by β-galactosidase activity assay. L, ONAC103L; S, ONAC103S. C. Schematic of the effector and reporter constructs used in the dual-luciferase reporter assays shown in (D–G). D-G. Dual-luciferase reporter assays revealing that ONAC103S inhibited the transcriptional activation activity of ONAC103L toward its target genes in rice protoplasts. The promoters of target genes *OsPAO* (D), *OsNOL* (E), *OsNAP* (F) and *OsNYC4*(G) were cloned into the reporter vector. Data are presented as means ± SD (n = 3). H-K. EMSA assays showing that ONAC103S inhibits the binding of ONAC103L to its target gene promoters, including *OsPAO*, *OsNOL*, *OsNAP*, and *OsNYC4*. Two-way ANOVA was performed to determine the statistical significance of differences in (B) and (D–G).

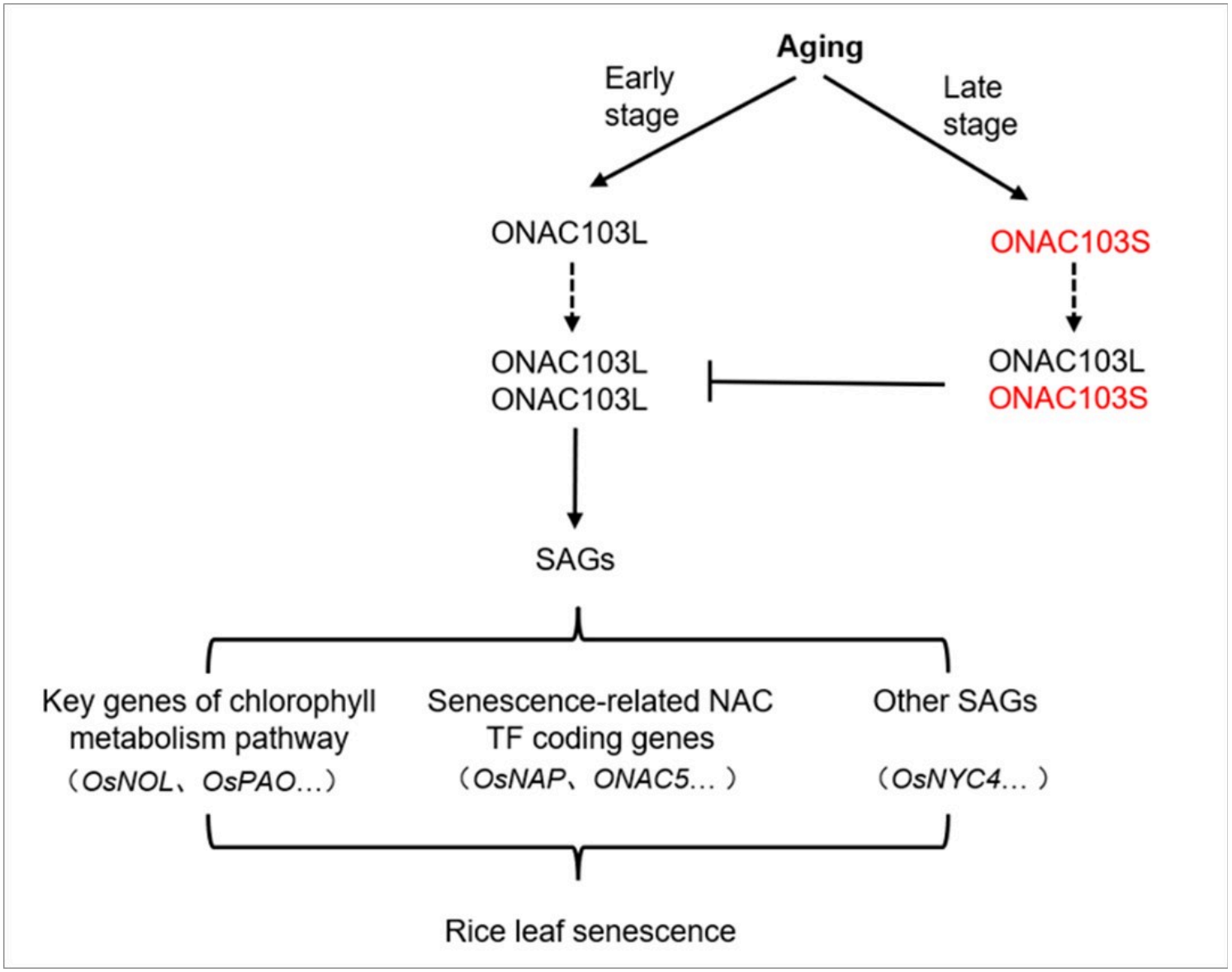


Figure 10

Proposed working model for the roles of ONAC103L and ONAC103S in regulating leaf senescence.

Supplementary Files

This is a list of supplementary files associated with this preprint. Click to download.

- CombinedSupplementalFigures.pdf